Molecular Cloning of cDNA Encoding an Aquaglyceroporin, AQP-h9, in the Japanese Tree Frog, Hyla japonica: Possible Roles of AQP-h9 in Freeze Tolerance

Authors: Hirota, Atsushi, Takiya, Yu, Sakamoto, Joe, Shiojiri, Nobuyoshi, Suzuki, Masakazu, et al.

Source: Zoological Science, 32(3) : 296-306

Published By: Zoological Society of Japan

URL: https://doi.org/10.2108/zs140246

ZOOLOGICAL SCIENCE **32**: 296–306 (2015)

Molecular Cloning of cDNA Encoding an Aquaglyceroporin, AQP-h9, in the Japanese Tree Frog, *Hyla japonica*: Possible Roles of AQP-h9 in Freeze Tolerance

Atsushi Hirota[1†], Yu Takiya[2†], Joe Sakamoto[1], Nobuyoshi Shiojiri[1,2], Masakazu Suzuki[1,2], Shigeyasu Tanaka[1,2], and Reiko Okada[1,2*]

[1]*Integrated Bioscience Section, Graduate School of Science and Technology, Shizuoka University, Shizuoka 422-8529, Japan*
[2]*Department of Biology, Graduate School of Science, Shizuoka University, Shizuoka 422-8529, Japan*

In order to study the freeze-tolerance mechanism in the Japanese tree frog, *Hyla japonica*, we cloned a cDNA encoding aquaporin (AQP) 9 from its liver. The predicted amino acid sequence of *H. japonica* AQP9 (AQP-h9) contained six putative transmembrane domains and two conserved Asn-Pro-Ala motifs, which are characteristic of AQPs. A swelling assay using *Xenopus laevis* oocytes injected with AQP-h9 cRNA showed that AQP-h9 facilitated water and glycerol permeation, confirming its property as an aquaglyceroporin. Subsequently, glycerol concentrations in serum and tissue extracts were compared among tree frogs that were hibernating, frozen, or thawed after freezing. Serum glycerol concentration of thawed frogs was significantly higher than that of hibernating frogs. Glycerol content in the liver did not change in the freezing experiment, whereas that in the skeletal muscle was elevated in thawed frogs as compared with hibernating or frozen frogs. Histological examination of the liver showed that erythrocytes aggregated in the sinusoids during hibernation and freezing, and immunoreactive AQP-h9 protein was detected over the erythrocytes. The AQP-h9 labeling was more intense in frozen frogs than in hibernating frogs, but nearly undetectable in thawed frogs. For the skeletal muscle, weak labels for AQP-h9 were observed in the cytoplasm of myocytes of hibernating frogs. AQP-h9 labeling was markedly enhanced by freezing and was decreased by thawing. These results indicate that glycerol may act as a cryoprotectant in *H. japonica* and that during hibernation, particularly during freezing, AQP-h9 may be involved in glycerol uptake in erythrocytes in the liver and in intracellular glycerol transport in the skeletal muscle cells.

Key words: aquaporin, aquaglyceroporin, hibernation, freeze tolerance, *Hyla japonica*

INTRODUCTION

A number of anuran species have adapted to cold climates by developing strategies against the repeated freezing and thawing of body fluids. Generally, freezing of body fluids results in various damaging effects, including high osmolality of the extracellular space, cell shrinkage, physical damages to the cell membrane, ischemia, and anoxia (Storey and Storey, 1984). To protect cells, freeze-tolerant frogs utilize solutes of small particle size as cryoprotectants. For instance, high concentrations of glucose are known to stabilize cell functions during freezing (Hillman et al., 2008). In the case of *Rana sylvatica*, just after freezing of the body surface, glucose synthesis is observed mainly from glycogen stored in the liver, and an increase in plasma glucose concentration was detected approximately 5 min after the initiation of freezing (Storey and Storey, 1984; Storey and Storey, 1985). Likewise, plasma glucose levels increase and glucose accumulation is facilitated in peripheral organs when *Hyla versicolor*, *Hyla chrysoscelis*, or *Pseudacris crucifer* were exposed to temperatures below the freezing point (Schmid, 1982; Layne and Lee, 1989; Costanzo et al., 1992).

In addition to glucose, glycerol plays an important role in freeze tolerance in some frogs belonging to the genus *Hyla* (Layne and Jones, 2001). It has been reported that *H. chrysoscelis* increases plasma glycerol levels and accumulates glycerol in the liver and skeletal muscle at high concentrations during cold acclimation (Layne and Jones, 2001). Glycerol transport can be mediated by aquaglyceroporins, which comprise a subfamily of aquaporins (AQPs). AQPs are a class of integral membrane proteins that form a selective water pore in the plasma membrane of various cells of animals, plants, and microorganisms (Zardoya, 2005; Benga, 2009; Ishibashi et al., 2011). With regard to vertebrates, AQPs are basically categorized into three subfamilies: 1) classical AQPs, 2) aquaglyceroporins, and 3) unorthodox AQPs (Ishibashi et al., 2011). Classical AQPs, e.g., AQP1 and AQP2, conduct only water, whereas

* Corresponding author. Tel. : +81-54-238-3091;
Fax : +81-54-238-3091;
E-mail: okada.reiko@shizuoka.ac.jp
† These authors contributed equally to this work.
doi:10.2108/zs140246

aquaglyceroporins, e.g., AQP3 and AQP9, transport small, uncharged solutes, such as glycerol and urea, in addition to water (Rojek et al., 2008). For *H. chrysoscelis*, two types of classical AQPs, AQP1 (HC-1) and AQP2 (HC-2) and an aquaglyceroporin, AQP3 (HC-3) have been identified by cDNA cloning (Zimmerman et al., 2007). Quantitative PCR analysis further showed that expression of these AQP mRNAs changes between warm and cold conditions, implying that multiple AQPs are involved in osmoregulation related to thermal acclimation (Zimmerman et al., 2007). However, information on the physiological roles of AQPs in cold acclimation of amphibians remains limited. The Japanese tree frog, *H. japonica*, is distributed in both the temperate and the subarctic zones, and can survive severe winter conditions (Amphibiaweb; http://amphibiaweb.org/, 2015). In the present study, we cloned a cDNA encoding *H. japonica* AQP9 (AQP-h9) and analyzed the molecular characteristics of this protein. The freeze-tolerance mechanism of *H. japonica* was further examined focusing on AQP-h9 as a glycerol transporter.

MATERIALS AND METHODS

Animals

Adult Japanese tree frogs, *H. japonica*, of both sexes were supplied by Oh-uchi Aquatic Animal Supply (Saitama, Japan). The frogs used in this study had a snout-vent length of approximately 3.0 cm and weighed approximately 2.8 g. For freezing experiments, non-hibernating frogs that had been captured in late November were kept in plastic containers with moistened moss, fed a diet of mealworms, and exposed to natural conditions of temperature and light cycle. The frogs hibernated from December to February and were used for the freezing experiment. Active tree frogs that were captured in April were kept under normal laboratory conditions and were fed mealworms for one week before sampling. All animal experiments were carried out in compliance with the Guide for Care and Use of Laboratory Animals of Shizuoka University.

Molecular cloning of AQP-h9 cDNA

Total RNA was extracted from the frog liver with TRIzol reagent (Life Technologies, Carlsbad, CA, USA). A total of 3 μg RNA was reverse transcribed at 37°C for 50 min in 20 μL reverse transcription (RT) buffer containing 0.5 mM dNTP, 2.5 pmol oligo-dT_{16} primer, 10 mM dithiothreitol, 20 U RNase inhibitor (Takara, Shiga, Japan), and 200 U Moloney-murine leukemia virus (M-MLV) reverse transcriptase (Life Technologies). Following RT, the reaction solution was inactivated by heating at 70°C for 15 min. To obtain the partial nucleotide sequence of *H. japonica* AQP-h9 cDNA, a set of PCR primers (sense, 5′-GGATCTGCAGCAGTTTTTGG-3′; antisense, 5′-ATAGCTGCTCCAAGCATAGG-3′) was designed based on the cDNA sequence of *Xenopus tropicalis* (accession number XM_002937673). The conditions of the PCR amplification were denaturation at 94°C for 2 min, followed by 30 cycles of denaturation at 94°C for 30 s, annealing at 60°C for 30 s, and extension at 72°C for 60 s. The PCR products were purified after agarose gel electrophoresis and were sequenced. After a central portion of AQP-h9 cDNA was obtained, 3′- and 5′-rapid amplification of cDNA ends (RACE) techniques were applied to determine the full-length sequence of AQP-h9 cDNA, as reported by Akabane et al. (2007). For 3′-RACE, 1 μg total RNA was reverse transcribed using oligo-dT-adaptor primer (5′-$(T)_{19}$-GACTCGAGTCGACATCGA-3′) and M-MLV reverse transcriptase (Life Technologies) in 20 μL reaction solution. A 1 μL aliquot of the RT product was then amplified by PCR with 3′-RACE primer (5′-TACAGCTCTGTTGCTCATGC-3′) and adaptor primer (5′-GACTCGAGTCGACATCGA-3′), followed by nested PCR using 3′-RACE nested primer (5′-CCAAGAATCTTTA-CAGCTC-3′) and the adaptor primer. For 5′-RACE, 500 ng total RNA was reverse transcribed using 5′-RACE primer (5′-ATGTCA-GAGCACAGTTCAGC-3′). After the first strand of cDNA was purified with a QIAquick PCR purification kit (QIAGEN, Hilden, Germany), a poly(A) tail was added to the 3′-terminus of the cDNA with terminal deoxynucleotidyl transferase (Toyobo, Osaka, Japan). A 5 μL aliquot of poly(A)-tailed cDNA was then amplified by PCR with the set of 5′-RACE and adaptor primers, followed by nested amplification using 5′-RACE nested primer (5′-AACAGCAACTG-GCTCTAGTC-3′) and the adaptor primer. The conditions of the PCR amplification for 3′- and 5′-RACE were denaturation at 94°C for 2 min, followed by 35 cycles of denaturation at 94°C for 30 s, annealing at 50°C for 30 s, and extension at 72°C for 90 s. The amplified products were purified and sequenced as described above.

Molecular phylogenetic analysis

The amino acid sequences of aquaglyceroporins from fish to human were aligned using Clustal W (Thompson et al., 1994). An optimal unrooted tree was inferred by the neighbor-joining method (Saitou and Nei, 1987) in the MEGA program ver. 5.0 (Tamura et al., 2011). The evolutionary distances were computed using the p-distance method (Nei and Kumar, 2000), and confidence in the neighbor-joining tree was assessed with 10,000 bootstrap replications (Felsenstein, 1985).

RT-PCR and quantitative real-time RT-PCR (qPCR) for AQP-h9 mRNA

Total RNA was extracted from *H. japonica* organs, i.e., the brain, heart, lung, stomach, intestine, liver, urinary bladder, kidney, fat body, skeletal muscle, and pelvic skin, and was reverse transcribed with the oligo-dT primer and M-MLV reverse transcriptase (Life Technologies), as described above. Specific primers for *H. japonica* AQP-h9 (sense, 5′-ATCCAGCAGTTTCGTTTGCG-3′; antisense, 5′-CAATGTTGACAGATACGGAGATGG-3′) and β-actin (AB092519) (sense, 5′-TGGCATCACACCTTCTACAATGAG-3′; antisense, 5′-TCACCAGAGTCCATCACGATACC-3′) were synthesized and used in PCR to amplify 227- and 215-bp products, respectively. RT-PCR was performed using TaKaRa Ex Taq (Takara) according to the manufacturer's instructions. The conditions of the PCR amplification were denaturation at 94°C for 1 min, followed by 30 cycles of denaturation at 94°C for 20 s, annealing at 65°C for 30 s, and extension at 72°C for 30 s. The amplified products were visualized on a 2% agarose gel containing ethidium bromide. Authenticity of PCR products was confirmed by sequencing. The qPCR assay was performed on LightCycler 480 (Roche Diagnostics, Tokyo, Japan) with 10 μL buffer containing 4 μL diluted cDNA, 0.5 μL of each of the primers (final concentration of 0.4 μM), 5 μL FastStart Essential DNA Green Master (Roche Diagnostics), and water in each well of a 384-well plate. The PCR program consisted of denaturation at 95°C for 5 min, and 45 cycles of denaturation at 95°C for 10 s, annealing at 65°C for 10 s, and extension at 72°C for 12 s. Following the cycle amplification, melting curve analysis was conducted from 65°C to 97°C to assess the specificity of PCR amplification. The qPCR assay was carried out in duplicate. The expression level of AQP-h9 mRNA was calculated according to a standard curve and normalized to β-actin mRNA using the LightCycler 480 multiple plate analysis software (Roche Diagnostics). Total RNA without RT was used as a negative control to check for contamination of genomic DNA, and water was used to check primer-dimer formation and reagent contamination.

Production of anti-AQP-h9 serum

A peptide corresponding to the amino acid residues 260–275 of AQP-h9 (ST-225; CIDIHDKKEPDHEMDP, Fig. 1) was synthesized as an antigen (Tanpaku Seisei Co., Gunma, Japan). Anti-

AQP-h9 antibody was raised in a rabbit immunized with the ST-225 peptide coupled to keyhole limpet hemocyanin (Pierce Biotechnology, Rockford, IL, USA), according to Tanaka and Kurosumi (1992).

Osmotic water and glycerol permeability of AQP-h9

A cDNA encoding the full-length AQP-h9 was produced by RT-PCR using a sense primer, consisting of a Kozak sequence and AQP-h9-specific sequence (5′-GCCACCATGAGGGAAAGGAGAAGCTG-3′), and antisense AQP-h9 primer (5′-$(T)_{25}$-ACAGTTCAGCAACGA-3′). The product of the PCR amplification was cloned into the pGEM-3Z vector (Promega, Madison, WI, USA). The pGEM-3Z vector containing the entire open reading frame (ORF) of AQP-h9 cDNA was linearized with *Eco*R I (Takara), and capped AQP-h9 cRNA was prepared with SP6 RNA polymerase (mCAP mRNA capping kit; Stratagene, La Jolla, CA, USA). *Xenopus laevis* oocytes at stages V–VI were defolliculated for 1 h with 1 mg/mL collagenase B (Roche Diagnostics) in sterile OR2 solution (100 mM NaCl, 2 mM KCl, 2 mM $MgCl_2$, and 5 mM Tris-HCl, pH 7.5). Isolated oocytes were microinjected with either cRNA (50 ng) in 50 nL DW or 50 nL DW and were incubated at 18°C for three days in Barth's buffer [88 mM NaCl, 10 mM KCl, 2.4 mM $NaHCO_3$, 1.7 mM $MgSO_4$, 0.48 mM $Ca(NO_3)_2$, 0.41 mM $CaCl_2$, and 7.6 mM Tris-HCl, pH 7.6, 200 mOsm] containing 10 μg/mL penicillin and 10 μg/mL streptomycin, after which they were transferred from 200 mOsm to 70 mOsm Barth's buffer (Saitoh et al., 2014; Shibata et al., 2014a, b) or to isotonic glycerol solution [130 mM glycerol, 23 mM NaCl, 10 mM KCl, 2.4 mM $NaHCO_3$, 1.7 mM $MgSO_4$, 0.48 mM $Ca(NO_3)_2$, 0.41 mM $CaCl_2$, and 7.6 mM Tris-HCl, pH 7.6, 200 mOsm] (Hansen et al., 2002). The osmotically-elicited increase in volume was monitored at 24°C under a BX50 microscope (Olympus, Tokyo, Japan) with a 4× objective lens and a charge-coupled device camera connected to a computer. The coefficient of osmotic water permeability (*Pf*) was calculated as reported previously (Zhang et al., 1990; Fushimi et al., 1993). Glycerol permeability (*Ps*) was estimated according to Carbrey et al. (2003). Some of the AQP-h9 cRNA-injected oocytes were incubated with 0.3 mM $HgCl_2$ for 10 min before transfer to 70 mOsm Barth's buffer. Expression of AQP-h9 protein in the cRNA-injected oocytes was confirmed by Western blotting and immunohistochemistry.

```
GTGATGTTTGAAGTTGACACCACCAAGGGTGACAGGCGGAGCAGCAAGTATAGCACTTTA      60
GACATGAGGGAAAGAAGAAGCTGTTTAGAAAAACTTGCTCTGAGGAACAGCCTGGCAAGG     120
   M  R  E  R  R  S  C  L  E  K  L  A  L  R  N  S  L  A  R       19
GAAACCTTGTCTGAGTTTTTTGGGACATGCCTGTTGGTAACCTTCACATGTTGTAGTATC     180
 E  T  L  S  E  F  F  G  T  C  L  L  V  T  F  T  C  C  S  I      39
GCTACAGCAGTTCTCAACTATGGATCTTCTGGAGGAACCTTGGGTGCTACTGTTGGCTGT     240
 A  T  A  V  L  N  Y  G  S  S  G  G  T  L  G  A  T  V  G  C      59
TCATTGGCAGTCACTATGGCAATCTACGCAAGTGGAGGAGTGTCAGGAGGCCACGTCAAT     300
 S  L  A  V  T  M  A  I  Y  A  S  G  G  V  S  G  G  H  V  N      79
CCAGCAGTTTCGTTTGCGATGAGTATGACTGGAAAGCTGCCATGGGTCAAACTTCCTTTC     360
 P  A  V  S  F  A  M  S  M  T  G  K  L  P  W  V  K  L  P  F      99
TACATAACAGCACAGTTCCTTGGAGCTATCACCGGATCTGCCGCTGTTTTTGGTGTTTAT     420
 Y  I  T  A  Q  F  L  G  A  I  T  G  S  A  A  V  F  G  V  Y     119
TATGATGCATTAATGGCATACTCAGGAGGAGTGTTTAGAGTAACTGGGCCAAATGCTACA     480
 Y  D  A  L  M  A  Y  S  G  G  V  F  R  V  T  G  P  N  A  T     139
GCTCAAATTTTTGCAACATATCCATCTCCGTATCTGTCAACATTGAATGGACTTGTTGAT     540
 A  Q  I  F  A  T  Y  P  S  P  Y  L  S  T  L  N  G  L  V  D     159
CAAATGATGTCTACAGCTCTGTTGCTCATGCTGATCTTTGCCATATTTGACAAAAAGAAC     600
 Q  M  M  S  T  A  L  L  L  M  L  I  F  A  I  F  D  K  K  N     179
ATGCCAGCACCAAAGGGACTAGAGCCAGTTGCTGTTGGGCTCCTCATTCTAACATTAGCC     660
 M  P  A  P  K  G  L  E  P  V  A  V  G  L  L  I  L  T  L  A     199
CTGTCTCTAGGATCCAACTGTGGAGCCGCTATGAACCCAGCCAGAGACTTAGGCCCAAGA     720
 L  S  L  G  S  N  C  G  A  A  M  N  P  A  R  D  L  G  P  R     219
ATCTTTACAGCTCTGGCTGGCTGGGGCCCTGAAGTTTTCACTGCTGGTGGTAGCTTTTGG     780
 I  F  T  A  L  A  G  W  G  P  E  V  F  T  A  G  G  S  F  W     239
TGGATCCCTGTGGTCGGACCAATGCTTGGAGCTGTAATCGGGTCCTACATATACATTCTT     840
 W  I  P  V  V  G  P  M  L  G  A  V  I  G  S  Y  I  Y  I  L     259
TGCATTGACATTCATCACAAGAAAGAGCCAGATCATGAAATGGATCCTGATCACTTTGAA     900
 C  I  D  I  H  H  K  K  E  P  D  H  E  M  D  P  D  H  F  E     279
AAACATGAACTTGCCAACATGACTGAAAAGCCTAAAACTCGTTGCTGAACTGTGCTCTGA     960
 K  H  E  L  A  N  M  T  E  K  P  K  T  R  C  *                 294
CATCTATGGGCTACGTGCTTTTGTGTGCATAGGCCAACTTGCCTTTCTTCTGTGAACATG    1020
GACCTTCTGTGATTGGTTTATGATGATGTAACTGGGAGCCATGACTTAACTAATTACCTA    1080
CAAAATTAGAAGTTAAAATTAAAACAAAATATGAGTTTTTTTTAAAGGTTCTCATTAGTA    1140
TTTTATTCCTAGCCTTCAATCTCAGACATAAAAGTATCAGGGGATAATCATAATGCCCCT    1200
TAATTGCTGGGCCATAAATTATCCTTCTTAATGAAGCACTAATGGACCATAGACTGGGTC    1260
ACAAAGGTATATGCAGGTAATTGGTCTTGTCATGCATTAATGTGTAATAACTGTGATCCA    1320
TCATCAATACCATTAAAATTTGCTGTGTGTTAAAATGATTTTACTGTCAGAGGCCAAGAA    1380
CTTCACTTCAGTAAGATGCTGTTTCCCATCTATGAGAAAATGTATGATGCGCTGCTATCA    1440
ATTATTCTGCTAGTGAGGTCAATTTGTAAAGCCATAAACATTCAGTATCTCACAACCACT    1500
CAAACCCACTGGGCTGGAAAAAGAGCTTTTAGAAACCTGCAAGATTTTCTGTAACTTCTC    1560
AAATATTATTGCTTCTAGGGTGACCTCTGTACATTGTTCAGTTACCCTCCTTAGTTATAA    1620
AATAAATACCAAGGAAATAAATGTTAAATTATTGTATATTTCTAATTTTAATTGTTAAAG    1680
AACAATTTCTTGCATTGTTTTAAATTCACAATAAATGTTTTAAATCAC                1728
```

Fig. 1. Nucleotide sequence of *Hyla japonica* AQP-h9 cDNA. The predicted amino acid sequence of the AQP-h9 protein is shown below the nucleotide sequence (accession number LC008216). Six putative transmembrane domains are underlined (TMHMM Server v. 2.0, http://www.cbs.dtu.dk/services/TMHMM/; Krogh et al., 2001), and two canonical Asn-Pro-Ala (NPA) motifs are outlined. The circle and triangle indicate a putative *N*-glycosylation site and a potential phosphorylation site for protein kinase C, respectively. The broken line indicates the positions of the specific AQP-h9 primers utilized for RT-PCR and qPCR. The shadowed region corresponds to the amino acid sequence of the AQP-h9 antigen peptide, ST-225. The asterisk indicates the termination codon. The AATAAA polyadenylation signal is double underlined.

Western blot analysis

The AQP-h9 cRNA- or DW-injected *X. laevis* oocytes were homogenized in a cell lysis buffer [50 mM Tris-HCl, 0.15 M NaCl, 1% (v/v) Triton X-100, 0.1 mg/mL phenylmethylsulfonyl fluoride, and 1 μg/mL aprotinin, pH 8.0] and were centrifuged at 16,000 × *g* for 10 min to remove insoluble materials. The protein was denatured at 37°C for 60 min in a denaturation buffer [3% (w/v) sodium dodecyl sulfate, 70 mM Tris-HCl, 11.2% (v/v) glycerol, 5% (v/v) 2-mercaptoethanol, and 0.01% (v/v) bromophenol blue, pH 6.8], subjected to electrophoresis on a 12% (w/v) polyacrylamide gel, and then transferred to an Immobilon-P membrane (Millipore, Billerica, MA, USA). The membrane was blocked in 2% (w/v) skim milk (Wako Pure Chemicals, Osaka, Japan). The proteins on the membrane were reacted with rabbit anti-AQP-h9 serum diluted at 1:2,000, followed by incubation with peroxidase-labeled donkey anti-rabbit IgG (Dako, Copenhagen, Denmark). Immunopositive bands were visualized using enhanced chemiluminescence Western blotting detection reagents (GE Healthcare, Buckinghamshire, UK). To check the specificity of the immunoreaction, an absorption test was performed using the antiserum preincubated with an excess amount (10 μg/mL) of the antigen

peptide.

Freezing experiment

H. japonica, hibernating at 2–10°C, were transferred into 50 mL polypropylene tubes filled with moistened moss. The tubes were submerged in a cooling bath (CP-300R, TAITEC, Saitama, Japan) at –4°C for 6 h. Following the freezing, some frogs were sampled as a frozen group. The remaining frogs were thawed at room temperature (approximately 23°C) for 1 h after the 6 h freezing, followed by sampling. More than 80% of the frogs survived the freezing experiment. The active frogs sampled in April and the hibernating frogs were used as comparative controls. The frogs of each group were dissected, and then the blood was collected from the heart using capillary tubes (Terumo, Tokyo, Japan). The liver and thigh muscle were excised, immediately frozen in liquid nitrogen, and stored at –80°C until measurement of glycerol content or RT-PCR analysis was conducted. The excised tissues were also fixed in a periodate-lysine-paraformaldehyde fixative (PLP: 2% paraformaldehyde, 75 mM L-lysine hydrochloride, and 10 mM sodium periodate in 0.1 M phosphate buffer, pH 7.4) at 4°C for 16 h and were used for immunohistochemical analysis.

Measurement of glycerol concentrations in the serum and tissue extract

The blood samples of the frogs were centrifuged at 450 × *g* at 4°C for 10 min. The sera were then collected and stored at –20°C until further use. Each tissue sample from the liver and muscle was homogenized in 400 μL of ice-cold 0.7 × phosphate buffered saline (PBS; 0.01 M sodium phosphate buffer and 0.14 M NaCl, pH 7.5). After centrifugation at 20,000 × *g* at 4°C for 10 min, the supernatant was collected and used to measure the glycerol content. Glycerol concentrations in the serum and tissue extract were determined with a free glycerol reagent (Sigma-Aldrich, St. Louis, MO, USA). After incubation of the reaction solution containing 80 μL reagent and 10 μL serum, tissue extract, or glycerol standard at 37°C for 30 min, absorbance at 562 nm was measured with a microplate reader (Molecular Devices, Sunnyvale, CA, USA). The glycerol concentration was calculated from a standard curve. The tissue content of glycerol was standardized by the protein amount of each tissue, which was determined with a Pierce BCA protein assay kit (Thermo Fisher Scientific, Waltham, MA, USA), according to the manufacturer's instructions.

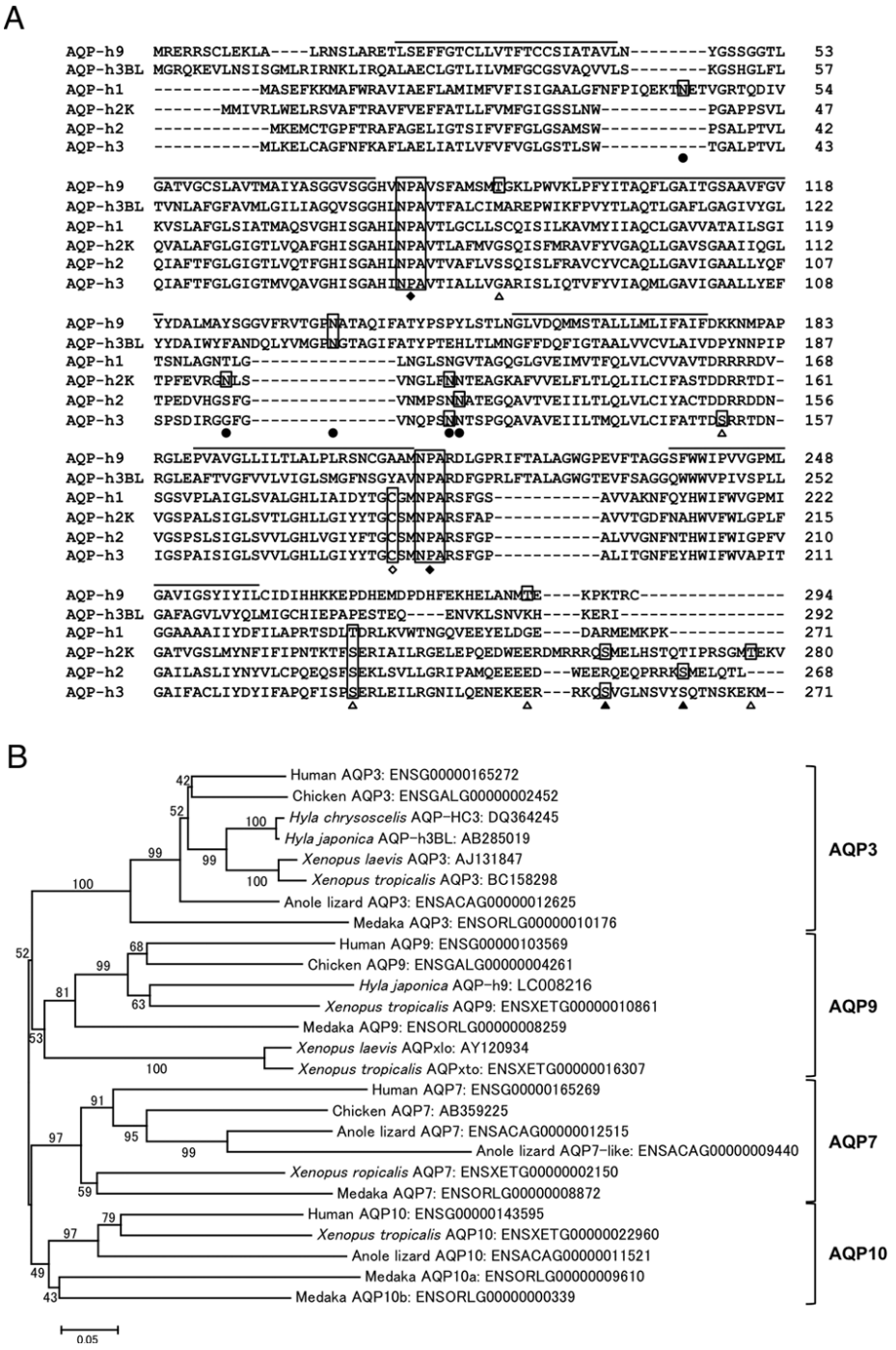

Fig. 2. Comparison between amino acid sequences of AQPs from *Hyla japonica* **(A)** and neighbor-joining unrooted tree of aquaglyceroporin proteins from fish to human **(B)**. **(A)** A pair of Asn-Pro-Ala (NPA) motifs (diamonds) are conserved in *H. japonica* AQPs; AQP-h9 (LC008216), AQP-h3BL (AQP3, BAF63030), AQP-h1 (AQP1, BAC07470), AQP-h2K (AQP2, BAF80993), AQP-h2 (AQPa2U, BAC82379; Shibata et al., 2014a), and AQP-h3 (AQPa2S, BAC07471; Shibata et al., 2014a). Six membrane-spanning domains are predicted in AQP-h9 (top lines), as in other AQPs. The circle, open triangle, and solid triangle indicate *N*-glycosylation sites, phosphorylation sites for protein kinase C, and phosphorylation sites for protein kinase A, respectively. Gaps marked by hyphens are inserted to optimize homology. **(B)** Aquaglyceroporins are divided into AQP3, AQP7, AQP9, and AQP10, and AQP-h9 is assigned into AQP9. Anuran-specific AQPxlo (Virkki et al., 2002) is also classified to AQP9, together with AQPxto (ENSXETG00000016307). The length of each branch is proportional to the mean number of differences per residue, and the numbers around the interior branches are bootstrap probabilities (percent; 10,000 replicates). The organism and accession number are indicated for each AQP.

Histology and immunofluorescence staining

The fixed liver and muscle were dehydrated through a graded ethanol series and were embedded in Paraplast plus (McCormick Scientific, St. Louis, MO, USA). Sections were prepared according to Nakakura et al. (2009). The sections were stained with Mayer's hematoxylin and eosin, dehydrated with ethanol, and then mounted in Entellan (Merck, Darmstadt, Germany). For immunofluorescence staining, the sections were covered with rabbit anti-AQP-h9 (1:1000) or rabbit anti-AQP-h3BL (1:2000; Akabane et al., 2007) for 16 h, followed by incubation with indocarbocyanine (Cy3)-labeled donkey anti-rabbit IgG (1:400; Jackson Immunoresearch, West Grove, PA, USA) for 2 h. For counterstaining of the nucleus, 4′, 6-diamidino-2-phenylindole (DAPI) was added to the secondary antibody solution. The specimens were washed in PBS and were mounted in PermaFluor (Thermo Fisher Scientific). The preparations were observed under an Olympus BX61 microscope equipped with a BX-epifluorescence attachment (Olympus). The specificity of immunostaining was checked using the antiserum that had been preincubated with 10 μg/mL of the antigen peptide.

Statistical analysis

Values were expressed as means ± SEM. The data were compared using Tukey's test. Statistical significance was set at $P < 0.05$.

RESULTS

Cloning of AQP-h9 cDNA

The nucleotide sequence and deduced amino acid sequence of *H. japonica* AQP-h9 cDNA are shown in Fig. 1. The cDNA consisted of 885 bp of a coding region, 63 bp of a 5′-untranslated region (UTR), and 780 bp of a 3′-UTR followed by a poly(A) tail. The ORF encoded a protein of 294 amino acid residues with the molecular mass calculated to be 31.5 kDa. As in other AQPs, certain features were conserved in AQP-h9; these were six transmembrane domains and a pair of canonical Asn-Pro-Ala (NPA) motifs at residues 79–81 and 211–213 (Figs. 1 and 2A). A putative *N*-linked glycosylation site and a potential phosphorylation site for protein kinase C were noted at Asn-137 and at Thr-287, respectively. AQP-h9 showed 20%, 21%, 44%, 19%, and 20% amino acid identity with AQP-h1 (Tanii et al., 2002), AQP-h2K (Ogushi et al., 2007), AQP-h3BL (Akabane et al., 2007), AQP-h2 (Hasegawa et al., 2003), and AQP-h3 (Tanii et al., 2002), respectively (Fig. 2A). On the other hand, AQP-h9 exhibited 59%, 56%, 55%, and 52% amino acid identity with *X. tropicalis* AQP9 (ENSXETG00000010861), chicken AQP9 (Sugiura et al., 2008), human AQP9 (Ishibashi et al., 1998), and medaka AQP9 (ENSORLG00000008259), respectively. Molecular phylogenetic analysis indicated that AQP-h9 forms the AQP9 cluster together with the AQP9 proteins of other vertebrates (Fig. 2B).

Expression of AQP-h9 mRNA

To investigate the distribution of AQP-h9 mRNA expression, RT-PCR was performed using specific primers. AQP-h9 mRNA expression was observed in all the organs tested, such as the brain, heart, lung, stomach, intestine, liver, urinary bladder, kidney, fat body, skeletal muscle, and pelvic skin (Fig. 3). Among these organs, AQP-h9 mRNA was expressed at relatively high levels in the liver, stomach, and pelvic skin.

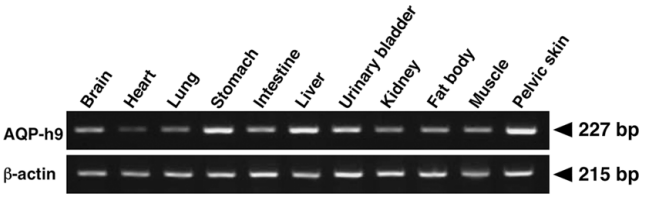

Fig. 3. AQP-h9 mRNA expression in various organs of *Hyla japonica*. RT-PCR products were separated on a 2% agarose gel and were stained with ethidium bromide. An amplified band for AQP-h9 mRNA was detected in all the tissues examined, including the liver and thigh muscle. β-actin mRNA was used as an internal control.

Water and glycerol permeation through AQP-h9

Transmembrane water flow through the AQP-h9 protein was evaluated by a swelling assay using *X. laevis* oocytes. Microinjected oocytes were incubated at 18°C for three days and were then transferred from isotonic (200 mOsm) to hypoosmotic (70 mOsm) Barth's buffer. The relative volume of the AQP-h9 cRNA-injected oocytes was markedly increased by hypotonic stimulation (Fig. 4A). The *Pf* value of the AQP-h9 cRNA-injected oocytes was approximately threefold higher than those that were injected with DW (Fig. 4B). The osmotic water permeability was inhibited by adding 0.3 mM $HgCl_2$ to incubation buffer (Fig. 4A, B). Effect of AQP-h9 on the glycerol permeability was analyzed by a swelling assay with isotonic (200 mOsm) glycerol solution (Fig. 4C, D). In this experimental system, glycerol enters the oocyte along the concentration gradient with a secondary influx of water, leading to oocyte swelling. Glycerol permeability in the AQP-h9 cRNA-injected oocytes was approximately fourfold higher than those injected with DW (Fig. 4D). Inhibition of the glycerol permeability was confirmed by adding 0.3 mM $HgCl_2$ to incubation buffer (Fig. 4C, D).

To evaluate whether the AQP-h9 protein was expressed in the cRNA-injected oocytes, sections of the AQP-h9 cRNA-injected oocytes were immunostained with anti-AQP-h9 (Fig. 4E). Immunopositive labeling was observed in the plasma membrane (Fig. 4E, a and b), agreeing well with the result of the swelling assay. The immunoreactivity was completely abolished by preabsorption of the antiserum with an excess amount of the immunogen peptide (Fig. 4E, c). No labeling was detected in the DW-injected oocytes (Fig. 4E, d). These results verified the specificity of the antibody. The expression of AQP-h9 protein in the oocytes was also examined by Western blot analysis. As shown in Fig. 4F, a band was detected at 31 kDa in an extract of AQP-h9 cRNA-injected oocytes (Fig. 4F, lane 1). The molecular mass of this protein was consistent with that predicted from the deduced amino acid sequence of AQP-h9. This band was not found in the DW-injected oocytes (Fig. 4F, lane 2) and vanished when the antiserum was preabsorbed with the antigen peptide (Fig. 4F, lane 3). These results confirm the specificity of the antibody and suggest that the band of 31 kDa represents AQP-h9.

Glycerol concentrations in the blood and tissues

The effects of freezing and/or thawing on the physiological condition of *H. japonica* were assessed by measuring the levels of glycerol in the serum, liver, and skeletal mus-

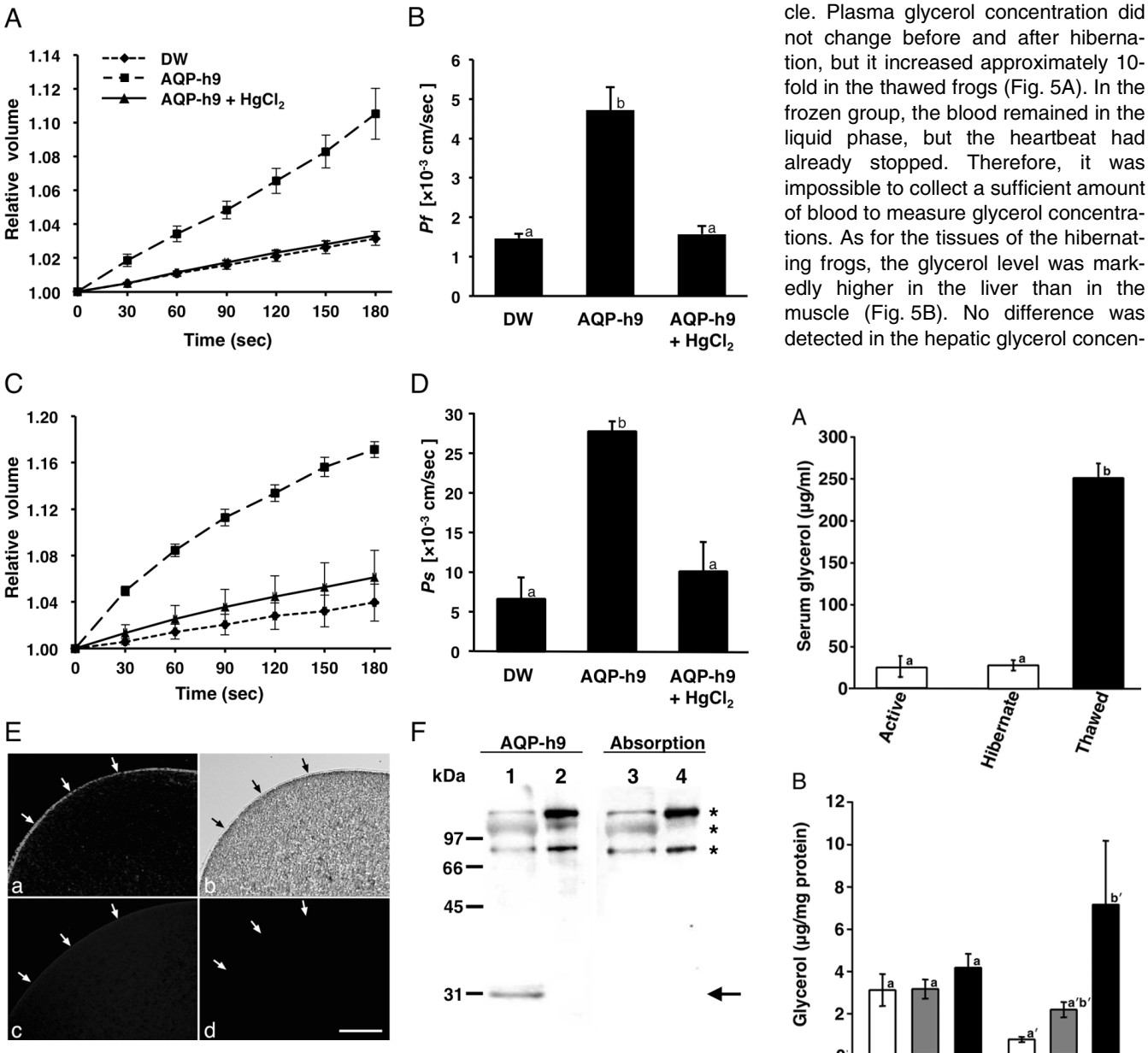

Fig. 4. Water and glycerol permeability analysis of AQP-h9 using *Xenopus laevis* oocytes. **(A)** Time course of the osmotic swelling by hypotonic stimulation. Oocytes were microinjected with DW or AQP-h9 cRNA. Some of the AQP-injected oocytes were incubated with 0.3 mM $HgCl_2$. **(B)** Osmotic water permeability (*Pf*) was calculated from the initial rate of oocyte swelling. Data are shown as the mean ± SEM (n = 6). Values with the different letters are significantly distinguishable from each other (Tukey's test, $P < 0.05$). **(C)** Time course of swelling in isotonic glycerol solution. Oocytes were microinjected with DW or AQP-h9 cRNA. Some of the AQP-h9-injected oocytes were incubated with 0.3 mM $HgCl_2$. **(D)** Glycerol permeability (*Ps*) was calculated from the initial rate of oocyte swelling. Data are shown as the mean ± SEM (n = 6). Values with the different letters are significantly distinguishable from each other (Tukey's test, $P < 0.05$). **(E)** Immunofluorescence images of AQP-h9 protein in the DW- or cRNA-microinjected oocytes. AQP-h9 immunoreactivity was intensively detected along the plasma membrane of the cRNA-injected oocytes (a); the Nomarski differential interference image corresponding to Fig. 4E, a (b); in the absorption test, immunoreactivity was abolished to background levels (c); and no immunopositive labels were observed in the DW-injected oocytes (d). Arrows indicate the plasma membrane. Scale bar = 100 μm. **(F)** Western blot analysis of the AQP-h9 cRNA- (lanes 1 and 3) or DW- (lanes 2 and 4) injected oocytes using anti-AQP-h9 serum (lanes 1 and 2) or anti-AQP-h9 serum preabsorbed with the antigen peptide (lanes 3 and 4). An arrow indicates an AQP-h9-specific band. Asterisks indicate non-specific signals.

cle. Plasma glycerol concentration did not change before and after hibernation, but it increased approximately 10-fold in the thawed frogs (Fig. 5A). In the frozen group, the blood remained in the liquid phase, but the heartbeat had already stopped. Therefore, it was impossible to collect a sufficient amount of blood to measure glycerol concentrations. As for the tissues of the hibernating frogs, the glycerol level was markedly higher in the liver than in the muscle (Fig. 5B). No difference was detected in the hepatic glycerol concen-

Fig. 5. Effects of freezing on glycerol concentrations in the serum **(A)** and tissue extracts **(B)** of *Hyla japonica*. **(A)** Serum glycerol concentration significantly increased when hibernating frogs were frozen and thawed. **(B)** Hepatic glycerol concentration did not change among the hibernating, frozen, and thawed frogs, whereas glycerol concentration of the thigh muscle significantly increased in the thawed frogs compared with the hibernating frogs. Data represent means ± SEM ($n = 7$). In each organ, values with the different letters are significantly distinguishable from each other (Tukey's test, $P < 0.05$).

trations among the hibernating, frozen, and thawed groups. By contrast, for the muscle, the glycerol concentration increased nearly 10-fold in the frozen frogs and about 50-fold in the thawed frogs as compared with the hibernating frogs (Fig. 5B).

Histology and immunohistochemistry for AQP-h9

Cytological features of the liver of *H. japonica* were first examined by traditional histochemical methods using hematoxylin and eosin. The parenchyma consisted of irregular cords or tubes of hepatocytes, forming internal intercellular bile canaliculi. Erythrocytes were observed in adjacent sinusoids and veins (Fig. 6A–D). After hibernation, the eosinophilic substance was lost, and the cytoplasm of hepatocytes was not densely stained except for hematoxyphilic materials

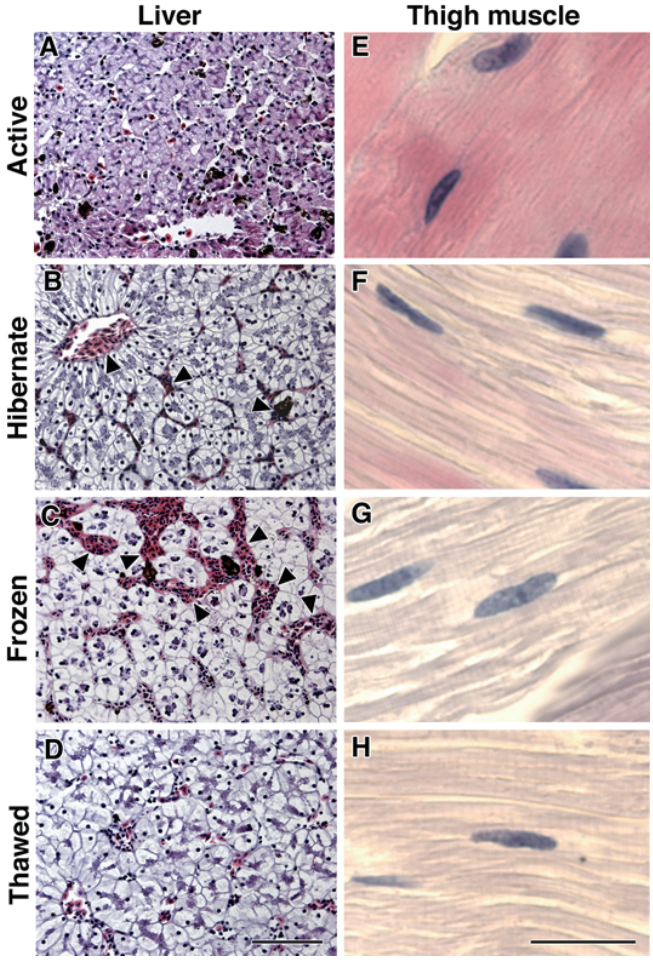

Fig. 6. Hematoxylin and eosin-stained images of the liver **(A–D)** and thigh muscle **(E–H)** in the active **(A, E)**, hibernating **(B, F)**, frozen **(C, G)**, and thawed **(D, H)** *Hyla japonica*. In the parenchyma of the liver, hepatocytes were arranged as irregular cords or tubes **(A–D)**. The cytoplasm of hepatocytes was densely stained in the active group **(A)**, but not in the other groups **(B–D)**. The erythrocyte clusters (arrowheads) were evident in the sinusoids of the hibernating group **(B)** and frozen group **(C)**. For the skeletal muscle, the cytoplasm of myocytes was stained in the active group **(E)**, but the staining was weaker in the other groups **(F–H)**. Myocyte atrophy was induced in the hibernating group **(F)** and progressed in the frozen group **(G)**. Scale bar **(A–D)** = 50 μm; **(E–F)** = 20 μm.

near the bile canaliculi (Fig. 6 B–D). Additionally, the erythrocytes aggregated in a sinusoidal net and veins (Fig. 6B). The erythrocyte clusters expanded in the frozen group (Fig. 6C) but were not clearly recognized in the thawed group (Fig. 6D). For the skeletal muscle, myocyte atrophy was observed after hibernation (Fig. 6F) and was more evident in the frozen group (Fig. 6G).

Immunofluorescence staining was then performed to examine the expression and localization of AQP-h9 in the liver and skeletal muscle. AQP-h9-immunoreactive signals were scarcely recognized in the liver of active frogs (Fig. 7A). Labels for AQP-h9 were detectable in erythrocytes in the liver of the hibernating frogs (Fig. 7C). Labels became more intense and located over the erythrocytes after freezing (Fig. 7E) but nearly disappeared in the thawed frogs (Fig. 7G). For the skeletal muscle, immunopositive labels for AQP-h9 were hardly detected in the active frogs (Fig. 8A), while weak labels were observed within myocytes in the hibernating frogs (Fig. 8C). AQP-h9 labeling was markedly enhanced in the frozen frogs (Fig. 8E) and was decreased in the thawed frogs (Fig. 8G). Immunoreactivity for AQP-h9 disappeared in the liver and muscle when the antiserum was preabsorbed with the antigen peptide (data not shown), confirming the specificity of the reaction. On the other hand, immunopositive AQP-h3BL was nearly undetectable in the liver or muscle in all the frog groups (data not shown).

Expression of AQP-h9 mRNA

With regard to the liver and thigh muscle, the mRNA expression of AQP-h9 was analyzed by RT-PCR and qPCR. AQP-h9 mRNA was intensely expressed in the liver and weakly expressed in the muscle (Fig. 9A). The expression levels of AQP-h9 mRNA in the liver and muscle were not changed by freezing or thawing (Fig. 9A and B).

DISCUSSION

In order to study the physiological roles of glycerol and aquaglyceroporins during freezing and thawing in *H. japonica*, we firstly determined the cDNA sequence of a *H. japonica* aquaglyceroporin AQP-h9, which was presumed to be a homolog of mammalian AQP9. Deduced amino acid sequence of *H. japonica* AQP-h9 contained six transmembrane domains and a pair of canonical NPA motifs as in other AQPs. The primary structure of *H. japonica* AQP-h9 showed a considerably high amino acid sequence similarity with those of other vertebrate animals, whereas relatively low sequence similarity was observed between AQP-h9 and other AQPs determined in *H. japonica.* These tendencies have also been observed in the case of another *H. japonica* aquaglyceroporin AQP-h3BL (Akabane et al., 2007).

AQP-h9 mRNA was revealed to be widely expressed in *H. japonica*, a relatively high expression being observed in stomach, liver, and pelvic skin. This agrees well with the expression pattern of AQP9 in mammals; this aquaglyceroporin is expressed in certain cell membranes of various organs such as testis, liver, brain, and skeletal myofiber (Inoue et al., 2009; Maeda, 2012).

As regard to the function of *H. japonica* AQP-h9 protein, it was evidenced that AQP-h9 facilitates water and glycerol permeation by the swelling assay using *X. laevis* oocytes injected with AQP-h9 cRNA. The result supports the notion

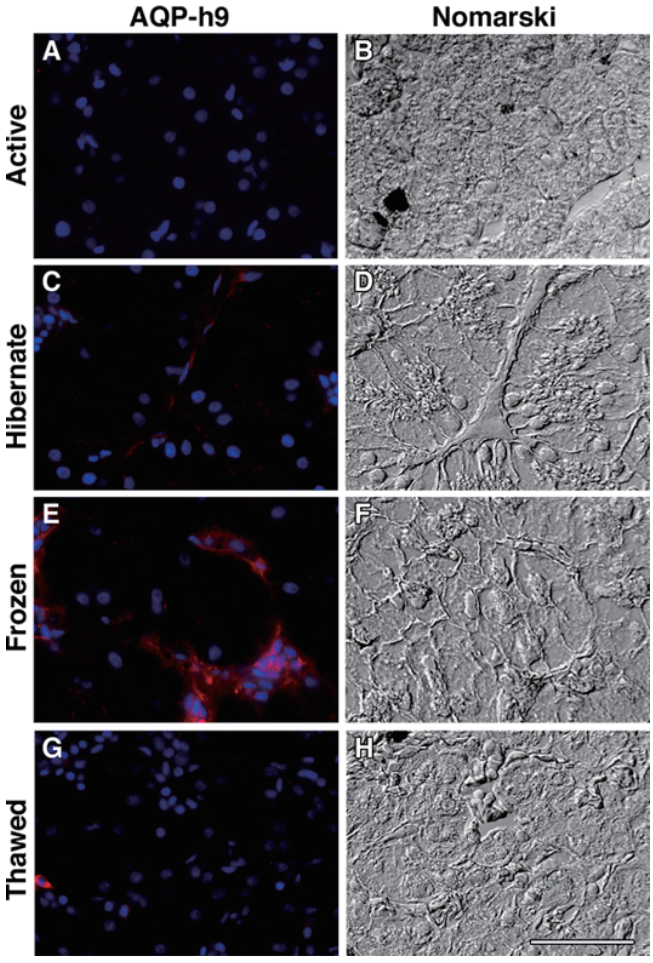

Fig. 7. Immunofluorescence images for AQP-h9 (red) in the liver of the active **(A)**, hibernating **(C)**, frozen **(E)**, and thawed **(G)** *Hyla japonica*. Nomarski differential interference-contrast images are shown as the corresponding references: **(B)** to **(A)**, **(D)** to **(C)**, **(F)** to **(E)**, and **(H)** to **(G)**. AQP-h9-immunopositive labels were scarcely detected in the liver of the active group **(A)**. In the hibernating group, erythrocytes were immunopositive for AQP-h9 **(C)**. In the frozen group, labeling was intensified and distributed over erythrocytes **(E)**. In the thawed group, labels almost disappeared, and few erythrocytes remained immunopositive **(G)**. Nuclei were counterstained with DAPI (blue). Scale bar = 50 μm.

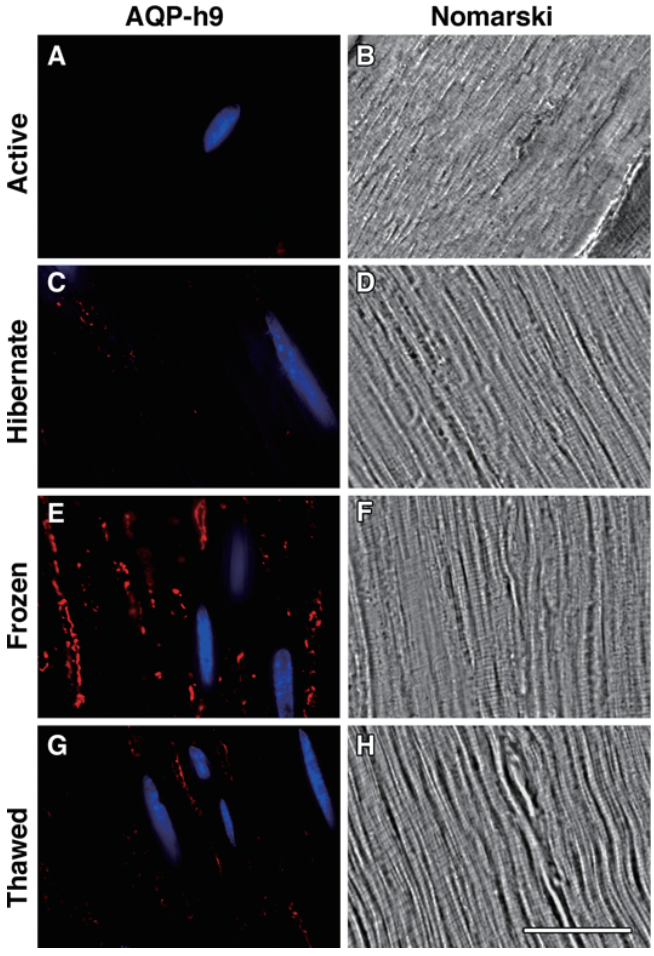

Fig. 8. Immunofluorescence images for AQP-h9 (red) in the thigh muscle of the active **(A)**, hibernating **(C)**, frozen **(E)**, and thawed **(G)** *Hyla japonica*. Nomarski differential interference-contrast images are shown as the corresponding references: **(B)** to **(A)**, **(D)** to **(C)**, **(F)** to **(E)**, and **(H)** to **(G)**. Immunopositive labels for AQP-h9 were scarcely observed in the muscle of the active group **(A)**. For the hibernating group, weak labels were distributed in the cytoplasm of myocytes **(C)**. Labeling was increased in the frozen group **(E)** and was reduced in the thawed group **(G)**. Nuclei were counterstained with DAPI (blue). Scale bar = 20 μm.

that the *H. japonica* AQP-h9 is a homolog of mammalian AQP9 and that AQP-h9 may be involved in water and glycerol transportations in various organs in *H. japonica.*

In the freezing experiment, serum glycerol concentration increased approximately 10-fold after the hibernating *H. japonica* were frozen and thawed. For the frozen frogs, a sufficient amount of blood could not be collected because of cardiac arrest; hence, exact glycerol levels were not determined. However, considering the high glycerol level in the serum of thawed frogs, it is likely that serum glycerol concentration is elevated by freezing and glycerol functioned as a cryoprotectant in the frozen frogs. In contrast, serum glycerol concentration in the hibernating *H. japonica* did not significantly differ from that in the frogs captured in April, suggesting that blood glycerol concentration is not increased by hibernation alone. Freezing and/or thawing of the body seem to be critical for increasing blood glycerol levels in *H. japonica*.

The present study revealed that during hibernation, glycerol concentration in *H. japonica* becomes higher in the liver than in the muscle. Although the liver glycogen is proposed to be a source of glycerol (Goldstein et al., 2010), no significant difference was detected in the hepatic glycerol concentrations among the hibernating, frozen, and thawed groups of *H. japonica*. In amphibians, the liver can supply glucose, another potential cryoprotectant, by glycogen breakdown and gluconeogenesis (Hillman et al., 2008), for which glycerol is a major substrate (Rodríguez et al., 2011). Provided that this occurs in frozen *H. japonica*, it may be one of the reasons why glycerol concentrations remain unchanged even when the animals were frozen and/or thawed.

In mammals, AQP9 localized at the sinusoidal plasma membrane facing the portal vein is known to mediate glyc-

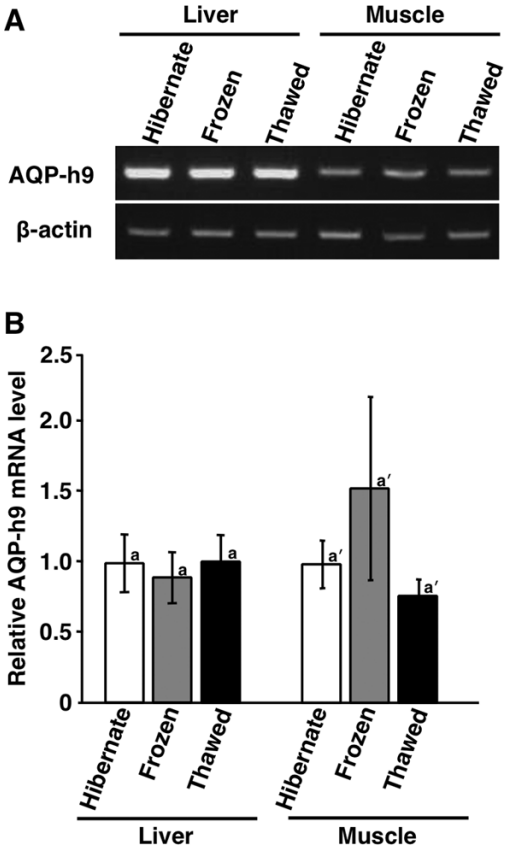

Fig. 9. Effects of freezing on expression of AQP-h9 mRNA in the liver and thigh muscle of *Hyla japonica*, examined by RT-PCR **(A)** and quantitative real-time RT-PCR **(B)**. **(A)** RT-PCR products were separated on a 2% agarose gel and were stained with ethidium bromide. Comparison of band intensities showed that AQP-h9 mRNA was expressed at higher levels in the liver than in the muscle. β-actin mRNA was used as an internal control. **(B)** The mRNA levels were measured according to the standard curve method of real-time PCR, and the expression levels of AQP-h9 mRNA were normalized to β-actin mRNA. For both the liver and muscle, AQP-h9 mRNA expression did not change among the hibernating, frozen, and thawed frogs. Data are shown as relative values to the hibernating group with the means ± SEM (n = 7). In each organ, values with the different letters are significantly distinguishable from each other (Tukey's test, $P < 0.05$).

erol entry into hepatocytes (Maeda, 2012). It would thus be plausible that AQP-h9 would also be located along the plasma membrane of hepatocytes in *H. japonica*. However, AQPh-h9 protein was not detected on the plasma membrane of hepatocytes in *H. japonica* in the present study. Five types of aquaglyceroporins, i.e., AQP3, AQP7, AQP9, AQP10, and anuran-specific AQPxto, are found in the genome of *X. tropicalis* (Fig. 2B) (Suzuki and Tanaka, 2010; Ensembl, http://ensemble.org/, 2014). Among them, mRNAs for AQP3, AQP9, and AQPxto have been detected in the liver of adult *X. tropicalis* by RT-PCR even after erythrocytes were removed from the liver by perfusion with saline (unpublished data). Given these findings, it may be that any one, or two, or all of other subtypes of AQP-h3BL and AQP9, and anuran-specific AQPxto-like protein are expressed in the hepatocytes of *H. japonica*, functioning as glycerol transporters. It should be mentioned, however, these AQPs have not been identified in this species. Accordingly, it remains to be elucidated which type of AQP is responsible for glycerol uptake in the hepatocytes in *H. japonica*.

Our immunohistochemical analysis of the liver showed that AQP-h9 is localized to the erythrocytes in the hibernating *H. japonica*. Moreover, it was found that its immunoreactivity becomes more intense by freezing and disappears after thawing. In mice, AQP1 and AQP9 have been detected in adult definitive erythroblasts and erythrocytes (Liu et al., 2007; Kingsley et al., 2013). It is known that erythrocytes from AQP9-null mice are defective in rapid glycerol transport across the plasma membrane, indicating that AQP9 constitutes the major pathway for glycerol transport in mouse erythrocytes (Liu et al., 2007). Given these lines of evidence, we speculate that this role of AQP9 has already been acquired in amphibians, contributing to the cryoprotection of erythrocytes when *H. japonica* frogs are exposed to freezing temperatures. According to Goldstein et al. (2010) and Mutyam et al. (2011), AQP3 is abundantly expressed in the erythrocytes of *H. chrysoscelis*. However, AQP3 (AQP-h3BL) was not detected in erythrocytes of *H. japonica*, suggesting the difference in the AQPs involved in the cryoprotection of erythrocytes due to the species difference.

For the skeletal muscle, glycerol concentration tends to increase in the frozen *H. japonica* and reaches the highest level in the thawed frogs. We further found that the AQP-h9 protein is expressed in myocytes and upregulated by freezing. Our immunochemical study, however, failed to localize AQP-h9 to the plasma membrane. For mammals, not only AQP9 but also AQP3 and AQP7 have been localized along the plasma membrane of skeletal muscle cells (Wakayama et al., 2002; Wakayama et al., 2004; Inoue et al., 2009). Hence, in *H. japonica*, glycerol transport across the sarcolemma might be mediated by aquaglyceroporins other than AQP9. Immunohistochemical analysis showed that AQP-h9 is distributed in the cytoplasm of myocytes, suggesting that AQP-h9 is located in intracellular vesicles, endoplasmic reticulum, and/or Golgi apparatus. It is therefore possible that AQP-h9 is involved in intracellular glycerol transport in myocytes during freezing.

To date, molecular biological studies with *H. chrysoscelis* have been conducted for AQPs including AQP1 (HC-1), 2 (HC-2), and 3 (HC-3) (Zimmerman et al., 2007; Goldstein et al., 2010; Pandey et al., 2010; Mutyam et al., 2011), but very little is known about the roles played by AQPs during adaptation to cold temperatures. Although AQP3 belongs to the aquaglyceroporin family, other aquaglyceroporins such as AQP7, 9, and 10 have not been tested for their involvement in adaptation to cold temperatures in any species of amphibians. In the present study, we examined physiological responses of the hibernating *H. japonica* to freezing and thawing, focusing on the roles of glycerol and AQP-h9. Our findings provide the first report on amphibian AQP9 in terms of its possible role in cryoprotection, functioning as an aquaglyceroporin. For a better understanding of the molecular mechanisms underlying freeze tolerance in *H. japonica,* however, further studies are definitely needed to elucidate the roles of other small solutes and their transporters as well as glycerol and aquaglyceroporins in cryoprotection.

ACKNOWLEDGMENTS

We express our sincere gratitude to Professor S. Kikuyama at Waseda University for his helpful comments and suggestion. We are very grateful to Dr. H. Mochida (Tanpaku Seisei Co.) for his generous technical assistance. This work was supported in part by Grants-in-Aid for Scientific Research from the Ministry of Education, Culture, Sports, Science and Technology of Japan to RO, MS, and ST (20570055; 23370028; 26440165).

REFERENCES

Akabane G, Ogushi Y, Hasegawa T, Suzuki M, Tanaka S (2007) Gene cloning and expression of an aquaporin (AQP-h3BL) in the basolateral membrane of water-permeable epithelial cells in osmoregulatory organs of the tree frog. Am J Physiol Regul Integr Comp Physiol 292: R2340–R2351

Benga G (2009) Water channel proteins (later called aquaporins) and relatives: past, present, and future. IUBMB Life 61: 112–133

Carbrey JM, Gorelick-Feldman DA, Kozono D, Praetorius J, Nielsen S, Agre P (2003) Aquaglyceroporin AQP9: solute permeation and metabolic control of expression in liver. Proc Natl Acad Sci 100: 2945–2950

Costanzo JP, Wright MF, Lee RE (1992) Freeze tolerance as an overwintering adaptation in Cope's grey treefrog (*Hyla chrysoscelis*). Copeia 1992: 565

Felsenstein J (1985) Confidence limits on phylogenies: an approach using the bootstrap. Evolution 39: 783–791

Fushimi K, Uchida S, Harat Y, Hirata Y, Marumo F, Sasaki S (1993) Cloning and expression of apical membrane water channel of rat kidney collecting tubule. Nature 361: 549–552

Goldstein DL, Frisbie J, Diller A, Pandey RN, Krane CM (2010) Glycerol uptake by erythrocytes from warm- and cold-acclimated Cope's gray treefrogs. J Comp Physiol B 180: 1257–1265

Hansen M, Kun JF, Schultz JE, Beitz E (2002) A single, bi-functional aquaglyceroporin in blood-stage *Plasmodium falciparum* malaria parasites. J Biol Chem 277: 4874–4882

Hasegawa T, Tanii H, Suzuki M, Tanaka S (2003) Regulation of water absorption in the frog skins by two vasotocin-dependent water-channel aquaporins, AQP-h2 and AQP-h3. Endocrinology 144: 4087–4096

Hillman SS, Withers PC, Drewes RC, Hillyard SD (2008) Ecological and Environmental Physiology of Amphibians. Oxford University Press, Oxford

Inoue M, Wakayama Y, Kojima H, Shibuya S, Jimi T, Hara H, et al. (2009) Aquaporin 9 expression and its localization in normal skeletal myofiber. J Mol Histol 40: 165–170

Ishibashi K, Kondo S, Hara S, Morishita Y (2011) The evolutionary aspects of aquaporin family. Am J Physiol Regul Integr Comp Physiol 300: R566–R576

Ishibashi K, Kuwahara M, Gu Y, Tanaka Y, Marumo F, Sasaki S (1998) Cloning and functional expression of a new aquaporin (AQP9) abundantly expressed in the peripheral leukocytes permeable to water and urea, but not to glycerol. Biochem Biophys Res Commun 244: 268–274

Kingsley PD, Greenfest-Allen E, Frame JM, Bushnell TP, Malik J, McGrath KE, et al. (2013) Ontogeny of erythroid gene expression. Blood 121: e5–e13

Krogh A, Larsson B, von Heijne G, Sonnhammer EL (2001) Predicting transmembrane protein topology with a hidden Markov model: application to complete genomes. J Mol Biol 305: 567–580

Layne JR, Jones AL (2001) Freeze tolerance in the gray treefrog: cryoprotectant mobilization and organ dehydration. J Exp Zool 290: 1–5

Layne JR, Lee RE (1989) Seasonal variation in freeze tolerance and ice content of the tree frog *Hyla versicolor*. J Exp Zool 249: 133–137

Liu Y, Promeneur D, Rojek A, Kumar N, Frøkiær J, Nielsen S, et al. (2007) Aquaporin 9 is the major pathway for glycerol uptake by mouse erythrocytes, with implications for malarial virulence. Proc Natl Acad Sci 104: 12560–12564

Maeda N (2012) Implications of aquaglyceroporins 7 and 9 in glycerol metabolism and metabolic syndrome. Mol Aspects Med 33: 665–675

Mutyam V, Puccetti MV, Frisbie J, Goldstein DL, Krane CM (2011) Dynamic regulation of aquaglyceroporin expression in erythrocyte cultures from cold- and warm-acclimated cope's gray treefrog, *Hyla chrysoscelis*. J Exp Zool A Ecol Genet Physiol 315A: 424–437

Nakakura T, Sato M, Suzuki M, Hatano O, Takemori H, Taniguchi Y, et al. (2009) The spatial and temporal expression of delta-like protein 1 in the rat pituitary gland during development. Histochem Cell Biol 131: 141–153

Nei M, Kumar S (2000) Molecular Evolution and Phylogenetics. Oxford University Press, Oxford

Ogushi Y, Mochida H, Nakakura T, Suzuki M, Tanaka S (2007) Immunocytochemical and phylogenetic analyses of an arginine vasotocin-dependent aquaporin, AQP-h2K, specifically expressed in the kidney of the tree frog, *Hyla japonica*. Endocrinology 148: 5891–5901

Pandey RN, Yaganti S, Coffey S, Frisbie J, Alnajjar K, Goldstein D (2010) Expression and immunolocalization of aquaporins HC-1, -2, and -3 in Cope's gray treefrog, *Hyla chrysoscelis*. Comp Biochem Physiol A Mol Integr Physiol 157: 86–94

Rodríguez A, Catalán V, Gómez-Ambrosi J, Frühbeck G (2011) Aquaglyceroporins serve as metabolic gateways in adiposity and insulin resistance control. Cell Cycle 10: 1548–1556

Rojek A, Praetorius J, Frøkiaer J, Nielsen S, Fenton RA (2008) A current view of the mammalian aquaglyceroporins. Annu Rev Physiol 70: 301–327

Saitou N, Nei M (1987) The neighbor-joining method: a new method for reconstructing phylogenetic trees. Mol Biol Evol 4: 406–425

Saitoh Y, Ogushi Y, Shibata Y, Okada R, Tanaka S, Suzuki M (2014) Novel vasotocin-regulated aquaporins expressed in the ventral skin of semiaquatic anuran amphibians: evolution of cutaneous water-absorbing mechanisms. Endocrinology 155: 2166–2177

Schmid WD (1982) Survival of frogs in low temperature. Science 215: 697–698

Shibata Y, Katayama I, Nakakura T, Ogushi Y, Okada R, Tanaka S, Suzuki M (2014a) Molecular and cellular characterization of urinary bladder-type aquaporin in *Xenopus laevis*. Gen Comp Endocrinol http://dx.doi.org/10.1016/j.ygcen.2014.09.001

Shibata Y, Sano T, Tsuchiya N, Okada R, Mochida H, Suzuki M, et al. (2014b) Gene expression and localization of two types of AQP5 in *Xenopus tropicalis* under hydration and dehydration. Am J Physiol Regul Integr Comp Physiol 307: R44–R56

Storey JM, Storey KB (1985) Adaptations of metabolism for freeze tolerance in the gray tree frog, *Hyla versicolor*. Can J Zool 63: 49–54

Storey KB, Storey JM (1984) Biochemical adaption for freezing tolerance in the wood frog, *Rana sylvatica*. J Comp Physiol B 155: 29–36

Sugiura K, Aste N, Fujii M, Shimada K, Saito N (2008) Effect of hyperosmotic stimulation on aquaporins gene expression in chick kidney. Comp Biochem Physiol A Mol Integr Physiol 151:173–179

Suzuki M, Tanaka S (2010) Molecular diversity of vasotocin-dependent aquaporins closely associated with water adaptation strategy in anuran amphibians. J Neuroendocrinol 22: 407–412

Tamura K, Peterson D, Peterson N, Stecher G, Nei M, Kumar S (2011) MEGA5: molecular evolutionary genetics analysis using

maximum likelihood, evolutionary distance, and maximum parsimony methods. Mol Biol Evol 28: 2731–2739

Tanaka S, Kurosumi K (1992) A certain step of proteolytic processing of proopiomelanocortin occurs during the transition between two distinct stages of secretory granule maturation in rat anterior pituitary corticotrophs. Endocrinology 131: 779–786

Tanii H, Hasegawa T, Hirakawa N, Suzuki M, Tanaka S (2002) Molecular and cellular characterization of a water-channel protein, AQP-h3, specifically expressed in the frog ventral skin. J Membr Biol 188: 43–53

Thompson JD, Higgins DG, Gibson TJ (1994) CLUSTAL W: improving the sensitivity of progressive multiple sequence alignment through sequence weighting, position-specific gap penalties and weight matrix choice. Nucleic Acids Res 22: 4673–4680

Virkki LV, Franke C, Somieski P, Boron WF (2002) Cloning and functional characterization of a novel aquaporin from *Xenopus laevis* oocytes. J Biol Chem 277: 40610–40616

Wakayama Y, Jimi T, Inoue M, Kojima H, Shibuya S, Murahashi M, et al. (2002) Expression of aquaporin 3 and its localization in normal skeletal myofibres. Histochem J 34: 331–337

Wakayama Y, Inoue M, Kojima H, Jimi T, Shibuya S, Hara H, et al. (2004) Expression and localization of aquaporin 7 in normal skeletal myofiber. Cell Tissue Res 316: 123–129

Zardoya R (2005) Phylogeny and evolution of the major intrinsic protein family. Biol Cell 97: 397–414

Zhang RB, Logee KA, Verkman AS (1990) Expression of mRNA coding for kidney and red cell water channels in *Xenopus* oocytes. J Biol Chem 265: 15375–15378

Zimmerman SL, Frisbie J, Goldstein DL, West J, Rivera K, Krane CM (2007) Excretion and conservation of glycerol, and expression of aquaporins and glyceroporins, during cold acclimation in Cope's gray tree frog *Hyla chrysoscelis*. Am J Physiol Regul Integr Comp Physiol 292: R544–R555

(Received October 30, 2014 / Accepted December 22, 2014)